Materials Research. 2023; 26:e20230127
DOI: https://doi.org/10.1590/1980-5373-MR-2023-0127

Applying ANOVA to Study the Effect of Weight Factions of the Nano-Hafnia Dispersed in Spin Coated Gelatin on the Corrosion Behaviour of AISI 316L Steel

Mohammed A. Almomani[a]*, Mohammed T. Hayajneh[a], Mohammad Y. Al-Daraghmeh[a]

[a]Jordan University of Science and Technology, Faculty of Engineering, Industrial Engineering Department, P.O. Box 3030, 22110, Irbid, Jordan.

Received: February 06, 2023; Revised: June 21, 2023; Accepted: August 16, 2023

This study aims to examine the potential improvement of uniform corrosion resistance and critical pitting potential of AISI 316L stainless steel (SS) in a simulated marine environment containing 3.5 wt. % NaCl by applying layer of gelatin containing HfO_2 nanoparticles using spin coating. Also, to examine the statistical significance of using different weight fractions of HfO_2 in the applied layer on the corrosion protection performance. The corrosion performance was assessed from potentiodynamic polarization. X-ray diffraction (XRD) was used to check the presence of HfO_2 in gelatin matrix. Scanning electron microscopy (SEM), and energy dispersive X-ray analysis (EDX) were used to examine the surface morphology and elemental composition of corrosion products. The results showed that the applied nanocomposite coatings enhanced both uniform and localized corrosion resistance of the underlying AISI 316L SS, also Analysis of Variance (ANOVA) test approved that the weight fractions of dispersed HfO_2 nanoparticles have a statistical significant effect on the corrosion performance. Nanocomposites coating having 2 wt.% of HfO_2 showed the best performance as compared to other examined coatings.

Keywords: *AISI 316L SS, uniform corrosion, critical pitting potential, gelatin nanocomposites, HfO_2 nanopartciles.*

1. Introduction

Nanocomposite coatings of polymer reinforced with inorganic ceramic nanoparticles have been used recently to enhance the corrosion resistance of the underlying metal substrate. They provide barriers for corrosive ions diffusion and penetration[1-6].

Gelatin is considered a promising candidate material in medical applications because of its high biocompatibility[7-9]. Therefore, it was used by several researchers as a matrix in many nanocomposite coatings containing ceramic powder to protect the medical grade steel AISI 316L against corrosion[3,5,6]. These coatings show good protection capability against corrosion in corrosive environments containing chlorine[10].

The high dielectric constant of hafnium dioxide (HfO_2) makes it a good choice in corrosion protection coatings[11-13]. HfO_2 films give superior protection performance against corrosion as compared to ZrO_2, TiO_2, Al_2O_3, ZnO, ZrO_2 atomic layer deposited films from the potential reactive etchants and solvents[14,15]. Plasma reactive sputter deposited HfO_2 nanolayer was used to protect 316L SS against corrosion. This layer improves the uniform corrosion resistance of the underlying 316L SS substrate and increases the pitting potential to a more noble value[16]. Over the last few years, HfO_2 thin films were successfully deposited using thermal and plasma-enhanced atomic layer methods to provide protection against corrosion over different kinds of metal substrates, i.e., copper and AZ23 magnesium alloy[14,17].

Corrosion rate (r) and critical pitting potential (CPP) represent two important electrochemical parameters measured from a polarization experiment. The former one highlights to the materials' protection against uniform corrosion, whereas the latter is related to localized corrosion resistance and refers to the minimum potential level at which the pits become stable and autocatalytic growth begins[18,19].

ANOVA is a simple, widely known statistical approach that is used to examine the statistical significance difference between the means across multiple groups[20]. This method has become very popular in materials engineering to assess variation in the material properties with either elemental composition[21] or processing parameters[22,23].

In this paper, ANOVA approach is conducted with the aim to examine the statistical significance of weight fractions of HfO_2 nanoparticles incorporated into gelatin matrix nanocomposite coatings on both corrosion rate and pitting potential of 316L SS substrate in a 3.5 wt.% NaC solution.

2. Materials and Methods

2.1. Preparation of AISI 316L stainless steel substrates

Test coupons of AISI 316L SS with a square shape and size of 55 mm x 55 mm were cut from 1 mm thick sheet. The supplier provided the following chemical compositional analysis for 316L SS as listed in Table 1, and it is not based on a chemical analysis of each coupon used in this case. These coupons were used as substrate for coatings. Prior to coating, the substrates were chemically etched, ultrasonic cleaned, and then dried. The chemical etching was conducted using a 70:30 solution of nitric acid (HNO_3) and hydrogen peroxide

*e-mail: maalmomani7@just.edu.jo

(H_2O_2). Hence, substrate surface roughness increased which enhanced the coatings adhesion to the underlying substrate. Thereafter, substrates were ultrasonic cleaned in two stages using acetone and deionized water to remove surface stains. Lastly, the hot air stream was used to dry off the cleaned substrates. Figure 1 presents a flow chart of the sequential steps that were used to prepare the substrates for coating.

2.2. Preparation of gelatin- HfO_2 coatings

In this research, HfO_2 nanoparticles (size of 61- 80 nm, purity 99.99%, US Research Nanomaterials Company) were dispersed at different wt.%. in gelatin (type A porcine skin, Mw= 50,000-100,000, Sigma). All four types of coatings were applied at the same spinning speed (500–2500 rpm), and the spinning time was chosen to be 15 seconds, in order to prepare the sol gel coating material. A crosslinking agent called 1-ethyl-3-[3-dimethylaminopropyl] carbodiimide (EDC) is used to join carboxyl groups to primary amines. It creates an amine-reactive intermediate when it combines with a carboxyl. Figure 2 presents a schematic diagram for the gelatin-HfO_2 nanocomposites sol gel preparation process, and then spin coatings on an AISI 316L substrate. Those steps were similar to those used for other coatings and published elsewhere[1-4].

2.3. Characterization of the nanocomposite coated substrates

Due to the strong dielectric properties of the produced nanocomposite coatings, the surface was sprayed with a thin layer of gold. Then, SEM was used to examine the surface morphology of the coated samples before the corrosion test to investigate the homogeneity and dispersion of the nanoparticles within the gelatin matrix, and after the corrosion test to examine and observe carefully the surface morphological changes occurred during polarization experiment. EDX was used to study the elemental composition of the substrate surface and corrosion products. SEM and EDX were conducted using SEM model FEI Quanta FEG 450 at Nanotechnology Institute of Jordan University of Science and Technology. To confirm the presence of HfO_2 nanoparticles within the gelatin coating on the AISI 316L SS substrate, Diffractometer Rigaku Ultima IV model was used to conduct XRD at the Pharmaceutical Research Center of Jordan University of Science and Technology. In order to develop an understanding of the roughness of the coatings, image of the surface topography of the created nanocomposites' surfaces was collected using an AISI-NT atomic force microscope (AFM) at the Nanotechnology Institute of the Jordan University of Science and Technology. To evaluate the performance of the produced coating in protecting underlying substrate against uniform and localized pitting corrosion, potentiodynamic polarization test was used. This test was conducted with the aid of Gamry potentiostat Ref 600 corrosion testing instrument that was connected with three electrodes flat cell. The cell used graphite as a counter and saturated calomel (SCE) as reference electrodes. For each coating type, three replicates were used in this test.

2.4. Statistical analysis

The weight fraction of HfO_2 nanoparticles dispersed in the gelatin matrix in the produced nanocomposites determines the coating type. Four different types of spin coating layers were applied on AISI 316L SS substrate. The coatings were given the symbols A, B, C, and D as listed in Table 2; hereafter; these symbols will be used in the manuscript to refer to the examined nanocomposite coatings.

The statistical significance of the examined samples coating type was measured using one-way ANOVA analysis by Minitab software (Version 18). Differences were chosen to be significant for P-value < 0.05.

3. Results and Discussion

3.1. Electrochemical corrosion investigation

Figure 3 shows the potentiodynamic polarization curves of AISI 316L coated with different weight percentages of HfO_2 nanoparticles dispersed in a gelatin matrix at 500 - 2500 rpm spinning speeds. In order to build confidence in the scientific validity of the results, three replicates were examined at each weight fraction of HfO_2. The variation of the corrosion rate and critical pitting potential between the samples examined at each level was shown in the bar chart with different colors in Figures 4 and 5, respectively. The mean value and the standard deviation of the three replicates at each level of weight fractions for each one of the measured parameters are listed in Table 3. Here, the difference in color just denotes an independent experiment; the use of a certain color in the illustration does not imply that all trials that used that color are similar, since every experiment was run independently and at random.

Table 1. Chemical composition of AISI 316L SS as provided by the supplier.

Element	Fe	Cr	Ni	Mo	Mn	Si	Cu	N	C	P	S
wt.%	68.94	16.70	10.17	2.10	1.38	0.32	0.31	0.05	0.02	0.02	0.003

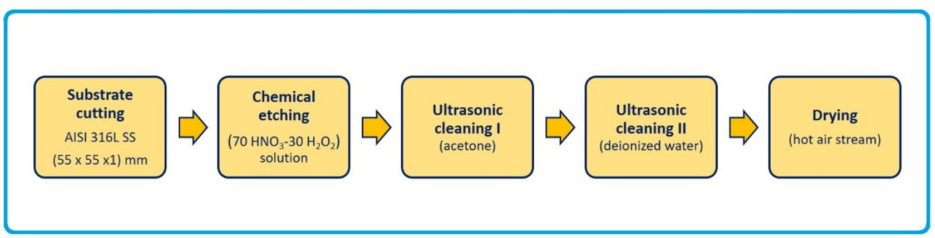

Figure 1. Flow chart of sequential steps used to prepare the substrates for coating.

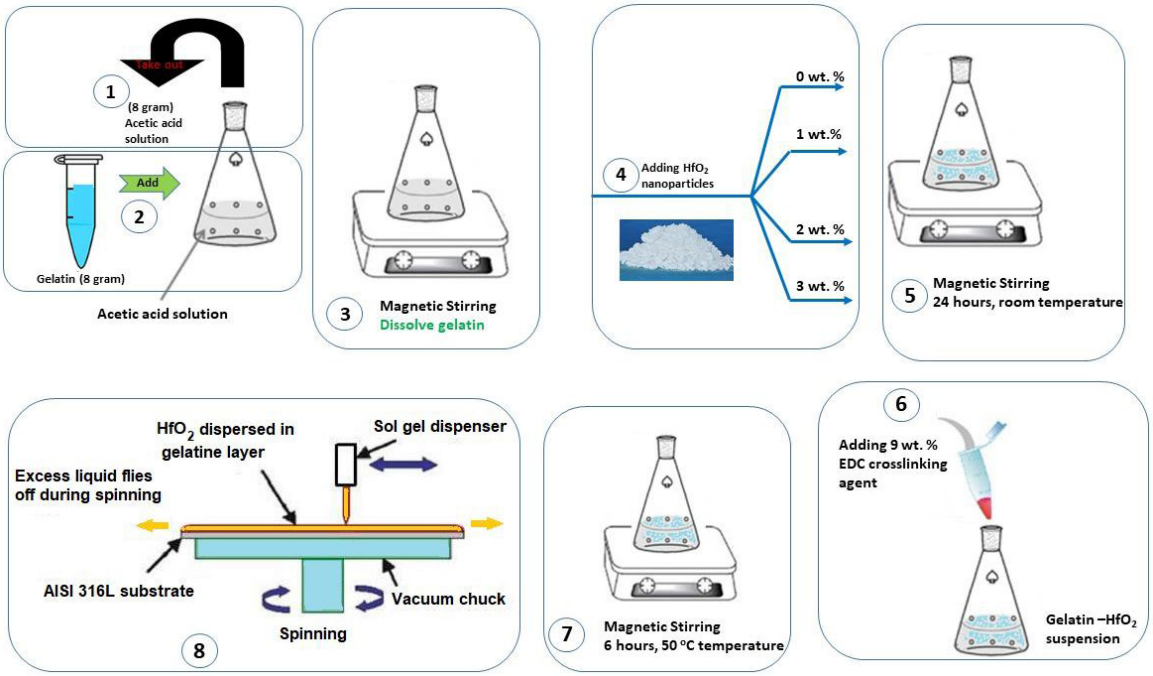

Figure 2. Schematic diagram for gelation-HfO_2 sol gel coating preparation steps.

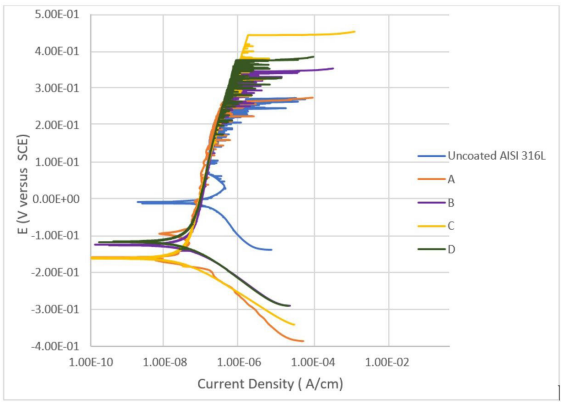

Figure 3. The potentiodynamic polarization curves of uncoated AISI 316L SS and samples with coating's type A, B, C, and D.

Table 2. The examined samples and HfO_2 weight fraction for each coating's type.

Coating type [a]	HfO_2 weight fraction [b]
Uncoated AISI 316 L	
A	0[c]
B	1
C	2
D	3

[a] Substrate: AISI 316L SS; [b] nanoparticles dispersed in gelatin matrix; [c] gelatin only.

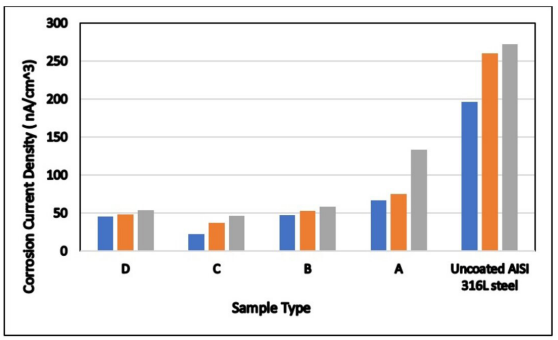

Figure 4. Corrosion Current Density (nA/cm^3) of uncoated AISI 316L SS and samples with coating's type A, B, C, and D.

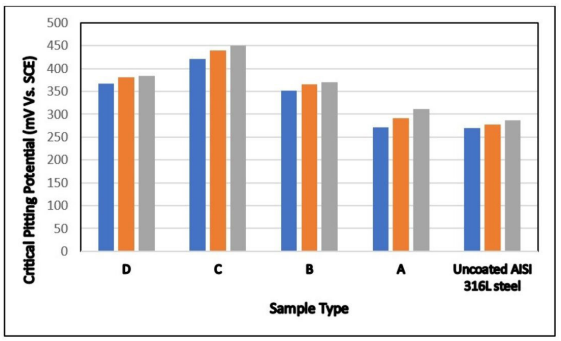

Figure 5. Critical pitting potential (mV vs. SCE) of uncoated AISI 316L SS and samples with coating's type A, B, C, and D.

The corrosion parameters that were obtained from the Tafel region of the examined samples include: corrosion potentials (E_{corr}), corrosion current densities (I_{corr}), and critical pitting potentials (E_{pit})[24]. The sample that has the least corrosion current density experienced the best corrosion resistance[25]. Thus, coating AISI 316L with gelatin reduces its' corrosion current density and thus its' corrosion rate. Also, dispersing HfO_2 nanoparticles in the gelatin reduced the corrosion

Table 3. Electrochemical parameters for the uncoated AISI 316L SS and samples with coating's type A, B, C, and D.

The Examined Samples "Coating's Type"	E_{corr} (mV vs. $SCE_{)}$	I_{corr} (nA/cm^2)	E_{pit} (mV vs. SCE)
Uncoated AISI 316 L	-43 ± 83	243 ± 33	278 ± 7
A	-129 ± 25	92 ± 29	291 ± 17
B	-117 ± 10	53 ± 5	359 ± 8
C	-128 ± 56	35 ± 10	437 ± 12
D	-144 ± 22	49 ± 4	377 ± 7

current density of the underlying AISI 316L substrate. The increase of pitting potential and shift to a higher noble value is a sign that the metastable pits that form during the anodic Tafel scan need higher potential to transform to stable pits. The curves show that no significant improvement on its' critical pitting potential was observed by coating AISI 316L SS with gelatin only. Nevertheless, dispersing HfO_2 nanoparticles in the gelatin increased the critical pitting potential significantly to more positive values. Where HfO_2 coating film provides a significant electrochemical corrosion protection and decreases the corrosion current density due its strong dielectric properties[14,26].

Figure 4 shows the effects of dispersing different weight fractions of HfO_2 nanoparticles on the corrosion current density of AISI 316L SS, dispersing 2 wt.% HfO_2 nanoparticles in gelatin outperform better than dispersing 3 wt. % of HfO_2 in gelatin, such behaviour can be attributed to the increase of tendency of nanoparticles to agglomerate in gelatin as the weight fraction percentage of nanoparticles increased, which increased the surface roughness. This will affect the corrosion current density adversely; these results are in agreement with previous research works[6].

Figure 5 shows the critical pitting potential behaviour of AISI 316L coated samples with different weigh percentages of HfO_2 nanoparticles (0,1, 2 and 3). It is shown that HfO_2 nanoparticles coating improved the critical pitting potential of the AISI 316L significantly, this behaviour is due to the formation of the stable coating layers on AISI 316L surface compared to the unstable oxide film on the uncoated AISI 316L, which could not sufficiently protect against pitting corrosion[6]. The change of critical pitting potential with weight fractions of HfO_2 are compatible with the corrosion current density results; where the highest electrochemical enhancement occurs at 2 wt. % HfO_2 nanoparticles coating due to the negative effect of agglomeration on surface roughness and critical pitting potential as well.

3.2. Statistical analysis

One-way ANOVA analysis with the significance level 95% was used to test the statistical significance of corrosion current density and critical pitting potential on the coating type. Minitab software (version 18) was utilized to conduct the test. Five levels of the examined coating type were used: uncoated AISI 316L SS, and samples of coatings (A, B, C, and D), each level has three replicates. Statistical procedures based on analysis of variance (ANOVA) methods were used to analyse the data. ANOVA test results for the effect of coating type on corrosion rate and critical pitting potential were summarized in Tables 4 and 5, respectively. The results confirmed that corrosion current density and the critical pitting potential are dependent on coating type. Therefore, the use of different coating type will affect significantly on both corrosion current density and critical pitting potential. It is shown that all coating types can improve the critical pitting potential of the uncoated AISI 316L significantly, this behaviour might be due to the formation of the stable coating layers on AISI 316L surface compared to the unstable oxide film on the uncoated AISI 316L, and the best electrochemical enhancement occurs at 2 wt. % HfO_2 nanocomposite coating. Hence, the statistical analysis is fully supported the electrochemical and morphology results. The individual value plot of the corrosion current Density (nA/cm^3) and the critical pitting potential (mV vs. SCE) of AISI 316L are graphically presented in Figure 6 and Figure 7.

Table 4. ANOVA test results of the samples **corrosion current density (I_{corr})** by the coating type.

Source	Df[a]	SS[b]	MS[c]	F[d]	P[e]
The Examined Sample	4	87860	21965	34.64	0.000
Error	10	6341	634		
Total	14	94201			

[a]Df = Degrres of Freedom; [b]Adj SS = Adjusted Sum of Squares; [c]Adj MS = Adjusted Means of Squares; [d]F-Value = Value on the F distribution; [e]P-Value = Value of the level of marginal significance

Table 5. ANOVA test results of the **critical pitting potential (E_{pit})** by the coating type.

Source	Df	SS	MS	F	P
The Examined Sample	4	51179	12794	72.61	0.000
Error	10	1762	176		
Total	14	52940			

3.3. Surface morphology and elemental composition analysis

3.3.1. Uncoated and coated AISI 316L SS with gelatin

The surface morphology of uncoated and coated AISI 316L SS with gelatin was examined previously and reported in our published work[3-5]. Prior to potentiodynamic polarization tests, only polishing lines appeared on the uncoated substrate surface; whereas autocatalytic stable pits were formed after polarization testing; the mechanism of these pits formation was described elsewhere[16]. Spin coating of AISI 316L SS with gelatin resulted in a smooth, uniform surface layer free of cracks and defects; however; after polarization this layer was cracked and failed to protect the underlying substrate. These results were in agreement with electrochemical polarization results that didn't show any improvement in the critical pitting potential of AISI 316L SS.

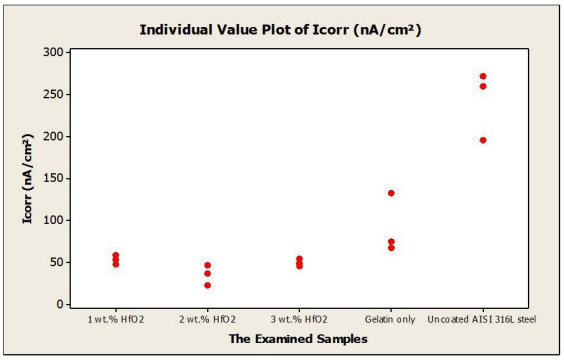

Figure 6. The individual value plot of the corrosion current Density (nA/cm^3) of uncoated AISI 316L SS and samples with coating's type A, B, C, and D.

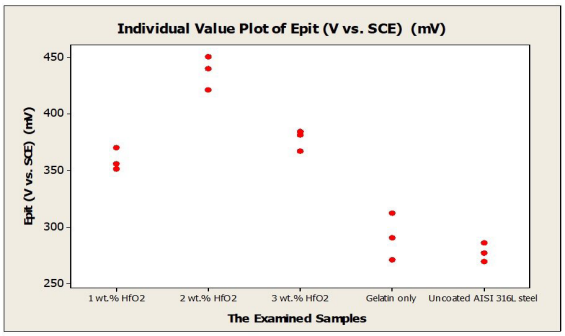

Figure 7. The individual value plot of the critical pitting potential (mV vs. SCE) of uncoated AISI 316L SS and samples with coating's type A, B, C, and D.

3.3.2. AISI 316L SS coated with HfO_2 nanoparticles dispersed in gelatin

Figure 8 shows SEM image of the sample of coating type C before conducting the polarization test. Nanoparticles were uniformly and homogeneously dispersed throughout the gelatin matrix, EDX spectrum for these dispersed particles is shown in Figure 9 and has peaks that belong to hafnium and oxygen (in addition to the substrate elements peaks), supporting the existence of HfO_2 nanoparticles.

On the other hand, the dispersion of HfO_2 nanoparticles in gelatin improves the coating's performance in protecting AISI 316L against corrosion. Figure 10 shows SEM image for the sample of coating type C after conducting the polarization, the surface was free of cracks and pits; the coating had nanoparticles similar to those observed in the coating prior to polarization experiments with small precipitates of salt. This is a decent indicator of the stability and functionality of this coating. Figure 11 shows an EDX spectrum of this sample; the spectrum had the substrate AISI 316L SS elements peaks. Also, hafnium, and oxygen peaks were observed, indicating that HfO_2 particles were not leached out. Sodium and chlorine peaks belong to precipitated salt on the surface.

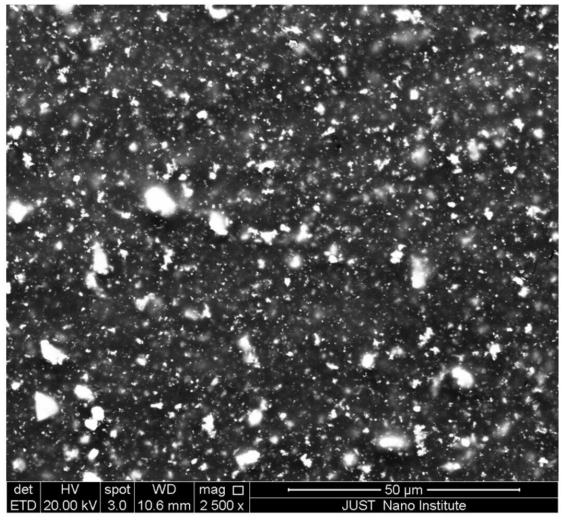

Figure 8. SEM image of the sample of coating type C before corrosion test.

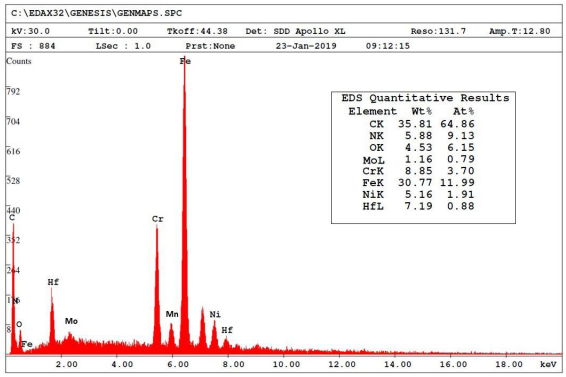

Figure 9. EDX spectrum of the sample of coating type C before corrosion test.

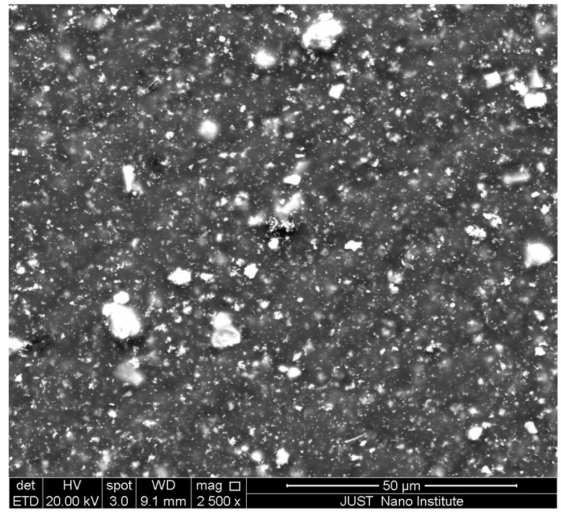

Figure 10. SEM image of the sample of coating type C after corrosion test.

3.4. XRD analysis

X-ray diffraction was used to confirm the existence of HfO_2 dispersed particle in the gelatin matrix of the produced nanocomposite coating. The XRD spectra for the uncoated 316L SS, and AISI 316L SS spin coated with HfO_2-gelatin nanocomposites are shown in Figure 12. XRD spectrum for AISI 316L SS substrate had three peaks belonging to

the austenitic phase and assigned to crystallographic planes (100), (200), and (220). The XRD spectrum of the coated sample was compared with the standard one and it confirmed the presence of m-HfO_2. All peaks are indexed accordingly.

3.5. AFM measurement

In order to develop an understanding of the roughness of the coatings, image of the surface topography of the sample of coating type C was collected using an AISI-NT atomic force microscope (AFM), and it is presented in Figure 13, showing that the average height of the coating is 10.57 µm.

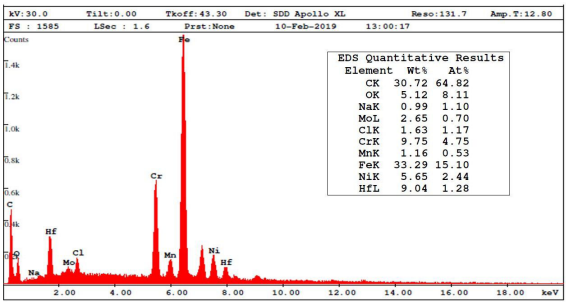

Figure 11. EDX spectrum of the sample of coating type C after corrosion test.

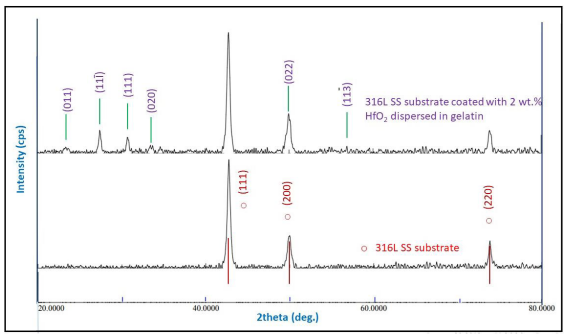

Figure 12. XRD spectra for uncoated AISI 316L SS and AISI 316L SS coated with coating C (2 wt.% HfO_2 dispersed in gelatin matrix).

4. Conclusions

This study aims to examine the potential improvement in the corrosion behaviour of AISI 316L SS achieved by applying layer of gelatin containing HfO_2 nanoparticles using spin coating technique in a simulated marine environment containing 3.5 wt.% NaCl. Based on the results of the study, the following points can be concluded:

- Coating AISI 316L with gelatin reduces its' corrosion current density and thus its' corrosion rate. However, no significant. improvement on it's critical pitting potential.
- Dispersing HfO_2 nanoparticles in the gelatin reduced the corrosion current density of the underlying AISI 316L substrate, and increase its pitting potential to more noble value.
- The gelatin coating containing 2 wt.% HfO_2 nanoparticles outperforms better than that containing 3 wt.% HfO_2 due to the high tendency of particles agglomeration at higher weight fraction, which increase the coating roughness.
- ANOVA test shows that the coating type (weight fraction of HfO_2) has a statistical significance effect on the performance of the applied coating in protecting the underlying AISI 316L SS substrate against uniform corrosion and localized pitting corrosion.

5. Acknowledgments

The authors would like to thank the Deanship of Scientific Research at Jordan University of Science and Technology (JUST) for supporting this work through grant no. 39/2017.

6. References

1. Almomani M, Hayajneh M, Al-Daraghmeh M. The corrosion behavior of AISI 304 stainless steel spin coated with ZrO_2 – gelatin nanocomposites. Mater Res Express. 2019;6(9):0965c4. http://dx.doi.org/10.1088/2053-1591/aaeea0.

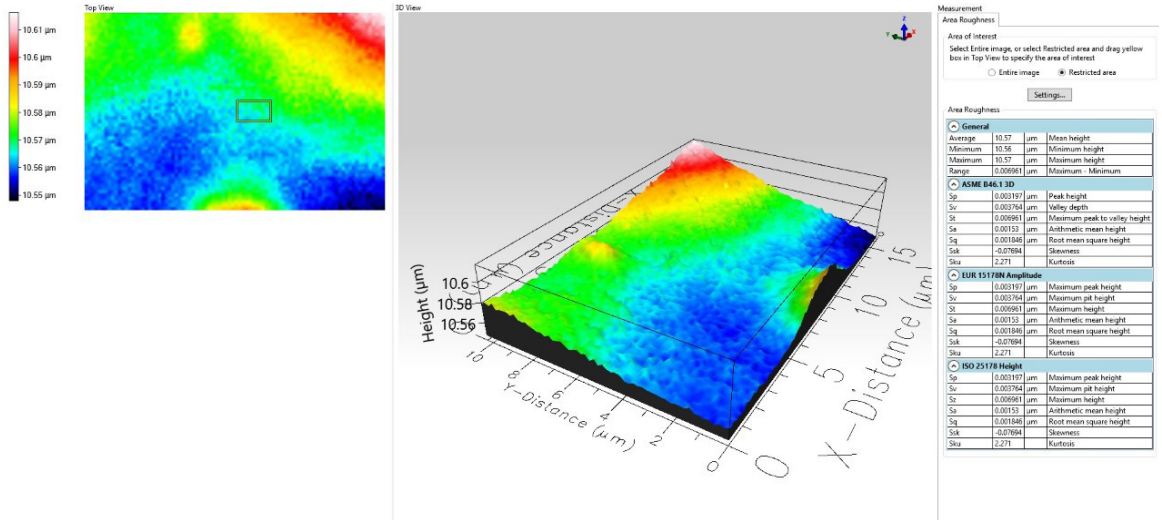

Figure 13. AFM image of the surface topography of the sample of coating type C.

2. Al-Daraghmeh M, Hayajneh M, Almomani M. Corrosion resistance of TiO_2-ZrO_2 nanocomposite thin films spin coated on AISI 304 stainless steel in 3.5 wt. % NaCl solution. Mater Res. 2019;22(5):e20190014. http://dx.doi.org/10.1590/1980-5373-mr-2019-0014.
3. Hayajneh M, Almomani M, Al-hmoud H. Corrosion evaluation of nanocomposite gelatin-forsterite coating applied on AISI 316L stainless steel. Mater Res Express. 2019a;6(11):ab49c3. http://dx.doi.org/10.1088/2053-1591/ab49c3.
4. Hayajneh M, Almomani M, Al-Daraghmeh M. Enhancement the corrosion resistance of AISI 304 stainless steel by nanocomposite gelatin-titanium dioxide coatings. Manuf Technol. 2019b;19(5):759-66. http://dx.doi.org/10.21062/ujep/368.2019/a/1213-2489/MT/19/5/759.
5. Hayajneh M, Almomani M, Al-Daraghmeh M. Development and evaluation of a thin cerium oxide-gelatin nanolaminate coating for corrosion protection of AISI 316L stainless steel. Manufacturing Technology. 2021;21(3):330-9. http://dx.doi.org/10.21062/mft.2021.036.
6. Torkaman R, Darvishi S, Jokar M, Kharaziha M, Karbasi M. Electrochemical and in vitro bioactivity of nanocomposite gelatin-forsterite coatings on AISI 316 L stainless steel. Prog Org Coat. 2017;103:40-7. http://dx.doi.org/10.1016/j.porgcoat.2016.11.029.
7. Chong E, Phan T, Lim I, Zhang Y, Bay B, Ramakrishna S, et al. Evaluation of electrospun PCL/gelatin nanofibrous scaffold for wound healing and layered dermal reconstitution. Acta Biomater. 2007;3(3):321-30. http://dx.doi.org/10.1016/j.actbio.2007.01.002.
8. Sakai S, Hirose K, Taguchi K, Ogushi Y, Kawakami K. An injectable, in situ enzymatically gellable, gelatin derivative for drug delivery and tissue engineering. Biomaterials. 2009;30(20):3371-7. http://dx.doi.org/10.1016/j.biomaterials.2009.03.030.
9. Zhong S, Zhang Y, Lim C. Tissue scaffolds for skin wound healing and dermal reconstruction. Wiley Interdiscip Rev Nanomed Nanobiotechnol. 2010;2(5):510-25. http://dx.doi.org/10.1002/wnan.100.
10. Djagny K, Wang Z, Xu S. Gelatin: a valuable protein for food and pharmaceutical industries. Crit Rev Food Sci Nutr. 2001;41(6):481-92. http://dx.doi.org/10.1080/20014091091904.
11. Mazur M, Poniedzialek A, Kaczmarek D, Wojcieszak D, Domaradzki J, Gibson D. Investigation of various properties of HfO_2-TiO_2 thin film composites deposited by multi-magnetron sputtering system. Appl Surf Sci. 2017;421:170-8. http://dx.doi.org/10.1016/j.apsusc.2016.12.129.
12. Perros A, Sippola P, Arduca E, Johansson L, Lipsanen H. Low temperature and high quality atomic layer deposition HfO_2 coatings. In: 2017 IMAPS Nordic Conference on Microelectronics Packaging (NordPac); 2017; Gothenburg, Sweden. Proceedings. New York: IEEE; 2017. p. 182-5. https://doi.org/10.1109/NORDPAC.2017.7993189.
13. Bright TJ, Watjen JI, Zhang ZM, Muratore C, Voevodin AA. Optical properties of HfO_2 thin films deposited by magnetron sputtering: from the visible to the far-infrared. Thin Solid Films. 2012;520(22):6793-802. http://dx.doi.org/10.1016/j.tsf.2012.07.037.
14. Daubert J, Hill G, Gotsch H, Gremaud A, Ovental J, Williams P, et al. Corrosion protection of copper using Al_2O_3, TiO_2, ZnO, HfO_2, and ZrO_2 atomic layer deposition. ACS Appl Mater Interfaces. 2017;9(4):4192-201. http://dx.doi.org/10.1021/acsami.6b13571.
15. Li M, Jin Z, Zhang W, Bai Y, Cao Y, Li W, et al. Comparisons of chemical stability and corrosion resistance of Group IV metal oxide films formed by thermal and plasma-enhanced atomic layer deposition. Sci Rep. 2019;9(1):10438. http://dx.doi.org/10.1038/s41598-019-47049-z.
16. Almomani M, Aita C. Pitting corrosion protection of stainless steel by sputter deposited hafnia, alumina, and hafnia-alumina nanolaminate films. J Vac Sci Technol A. 2009;27(3):449-55. http://dx.doi.org/10.1116/1.3100216.
17. Staišiūnas L, Leinartas K, Juzeliūnas E, Bučinskiene D, Grigucevičiene A, Kalinauskas P, et al. Anticorrosion performance of hafnium oxide ultrathin films on AZ31 magnesium alloy. Surf Coat Tech. 2020;397:126046. http://dx.doi.org/10.1016/j.surfcoat.2020.126046.
18. Frankel GS. Pitting corrosion of metals: a review of the critical factors. J Electrochem Soc. 1998;145(6):2186-98. http://dx.doi.org/10.1149/1.1838615.
19. Jones D. Principles and preventions of corrosion. 2nd ed. Essex: Pearson; 1995.
20. Montgomery D, Runger G. Applied statistics and probability for engineers. 7th ed. New York: Wiley; 2018.
21. Bataineh O, Almomani M. Applying ANOVA and DOE to study the effect of manganese on the hardness and wear rate of artificially aged Al-4.5wt%Cu alloys. Int J Cast Met Res. 2018;31(1):56-63. http://dx.doi.org/10.1080/13640461.2017.1366128.
22. Almomani M, Hayajneh M, Alelaumi S. Applying Taguchi method to study the wear behaviour of ZA-27 alloy-based composites reinforced with SiC nanoparticles. Int J Cast Met Res. 2019;32(4):229-41. http://dx.doi.org/10.1080/13640461.2019.1643061.
23. Hassan A, Almomani M, Qasim T, Ghaithan A. Statistical analysis of some mechanical properties of friction stir welded aluminium matrix composite. Int J Exp Des Process Optim. 2012;3(1):91-109. http://dx.doi.org/10.1504/IJEDPO.2012.045616.
24. Almomani M, Tyfour W, Nemrat M. Effect of silicon carbide addition on the corrosion behavior of powder metallurgy Cu-30Zn brass in a 3.5 wt.% NaCl solution. J Alloys Compd. 2016;679:104-14. http://dx.doi.org/10.1016/j.jallcom.2016.04.006.
25. Lim CYH, Lim CS, Gupta M. Wear behavior of SiCp-reinforced magnesium matrix composites. Wear. 2003;255(1-6):629-37. http://dx.doi.org/10.1016/S0043-1648(03)00121-2.
26. Fusco M, Woodward I, Oldham C, Parsons G. Enhanced corrosion protection of copper in salt environments with nanolaminate ceramic coatings deposited by atomic layer deposition. ESC Transactions. 2018;85(13):683-91. http://dx.doi.org/10.1149/08513.0683ecst.